

# Gravitational waves from the high temperature electroweak symmetry nonrestoration

Xiu-Fei Li<sup>\*</sup>*School of Physical Science and Technology, Inner Mongolia University, Hohhot 010021, China*
 (Received 4 January 2023; accepted 5 May 2023; published 24 May 2023)

The high temperature electroweak symmetry nonrestoration (SNR) opens a window to realize baryogenesis at high energy scales, which can alleviate the tight phenomenological constraints. An effective way to realize the electroweak SNR is to extend the Standard Model (SM) by adding a second Higgs doublet and a few new singlet fermions which interact with the second Higgs through a five-dimension operator. In this scenario, the second Higgs has a nonvanishing vacuum expectation value above the electroweak scale and thus breaks the electroweak symmetry. As the temperature decreases, the SM electroweak phase transition occurs and the Universe is located at SM electroweak vacuum. We show that the electroweak phase transition is the first order and the gravitational waves (GWs) generated during this process can be detected by the future GW experiments such as LISA, TianQin, DECIGO, and BBO.

DOI: [10.1103/PhysRevD.107.095034](https://doi.org/10.1103/PhysRevD.107.095034)

## I. INTRODUCTION

The first direct detection of gravitational wave (GW) by LIGO [1] in 2015 marked the beginning of GW astronomy. Most of the GWs come from violent astronomical processes such as black hole and neutron star binaries. These are important for the discovery of new astrophysical objects. The detection of GW is also significant to cosmology and high energy physics [2]. There are many potential cosmological sources for the stochastic GW backgrounds, such as inflation [3], reheating followed by inflation [2], cosmic string [4] and the first order cosmological phase transitions [5,6]. Since the GW can propagate freely once they are generated, one can use them to investigate the early Universe before the big bang nucleosynthesis [2]. Here, we focus on the first order cosmological phase transition.

In the Standard Model (SM), the electroweak phase transition and QCD phase transition are both crossovers. However, in many models beyond the SM, a first order phase transition is very common. For instance, extending the SM with one real scalar singlet, the Universe may experience a first order electroweak phase transition [7]. This suggests that the thermal history of the early Universe may be more exotic than the conventional scenario predicted by SM. An interesting example is that the electroweak symmetry may be nonrestoration (SNR) above the electroweak scale [8–20]. Recently, the high temperature SNR aroused great concern [21–32], because it opens a window to realize baryogenesis at high energy scales, which can alleviate the tight phenomenological constraints [22,23,26,32].

In this work, we study the high temperature electroweak SNR and the correlated GW signals in the two Higgs double model (2HDM). Here, the second Higgs  $H_2$  interacts with  $N_f$  new fermions  $\chi$  through a five-dimension operator  $\frac{1}{\Lambda}|H_2|^2\bar{\chi}\chi$  where  $\Lambda$  is the effective cutoff scale. This SNR term was first proposed in Refs. [24,29] and it can contribute a large negative thermal mass to  $H_2$  at high temperature. As a result,  $H_2$  acquires a large vacuum expectation value at high temperature, which breaks the electroweak symmetry. When the temperature of the Universe drops to electroweak scale, the SM electroweak phase transition occurs. We will show it is a first order phase transition and also discuss the GWs emitted during this process.

The paper is organized as follows. In Sec. II, we introduce the model. In Sec. III, we discuss the SNR and finite temperature effective potential. In Sec. IV, we study the first order electroweak phase transition and GWs. Finally, we summarize our results in Sec. V.

## II. THE MODEL

We extend the SM by adding second Higgs  $H_2$  and  $N_f$  new singlet fermions  $\chi$  which interact with the second Higgs through a five-dimension operator. Thus the new fermions have a Higgs-dependent mass term [24,29]

$$\mathcal{L} = -m_\chi^{(0)}\bar{\chi}\chi + \frac{1}{\Lambda}|H_2|^2\bar{\chi}\chi, \quad (1)$$

where  $m_\chi^{(0)}$  is the fermions bare mass and  $\Lambda$  is the effective cutoff scale. In this model, the  $\mathbb{Z}_2$  symmetric potential is given by [26]

---

<sup>\*</sup>xiufeili@imu.edu.cn

$$V(H_1, H_2) = -\mu_{h_1}^2 |H_1|^2 + \mu_{h_2}^2 |H_2|^2 + \lambda_{h_1} |H_1|^4 + \lambda_{h_2} |H_2|^4 + \lambda_m |H_1|^2 |H_2|^2, \quad (2)$$

where we neglected the term  $(H_1^\dagger H_2)(H_2^\dagger H_1)$  by assuming a custodial symmetry and an additional  $U(1)$  symmetry [26].  $H_1$  is the SM Higgs and  $H_2$  is the second Higgs,

$$H_1 = \frac{1}{\sqrt{2}} \begin{pmatrix} \sqrt{2}G^+ \\ h_1 + iG^0 \end{pmatrix}, \quad H_2 = \frac{1}{\sqrt{2}} \begin{pmatrix} \sqrt{2}h^+ \\ h_2 + ih^0 \end{pmatrix}. \quad (3)$$

Here  $G^\pm$  and  $G^0$  are the SM Goldstone bosons.  $h^\pm$  and  $h^0$  are the Goldstone bosons corresponding to the second Higgs. Then we can get the tree level effective potential

$$V(h_1, h_2) = -\frac{1}{2}\mu_{h_1}^2 h_1^2 + \frac{1}{2}\mu_{h_2}^2 h_2^2 + \frac{1}{4}\lambda_{h_1} h_1^4 + \frac{1}{4}\lambda_{h_2} h_2^4 + \frac{1}{4}\lambda_m h_1^2 h_2^2. \quad (4)$$

### III. SNR AND FINITE TEMPERATURE EFFECTIVE POTENTIAL

To illustrate the high temperature symmetry breaking or SNR, we first give a simple example, extending the SM with a gauge-singlet real scalar field  $S$  which has  $O(N_s)$  symmetry and couples to the SM via a Higgs portal. Then the scalar potential is

$$V_{\text{tree}} = V_{\text{SM}} + \frac{\mu_s^2}{2} S^2 + \frac{\lambda_s}{4} (S^2)^2 + \frac{\lambda_{hs}}{2} |H|^2 S^2, \quad (5)$$

where  $S^2 = S^T S$  and  $H$  is the SM Higgs doublet. The coupling  $\lambda_{hs}$  can be negative, as long as the vacuum stability condition

$$2\sqrt{\lambda_h \lambda_s} + \lambda_{hs} > 0. \quad (6)$$

In high temperature, the Higgs thermal mass has the form

$$\Pi_h(T) \approx \left( \frac{\lambda_h}{2} + \frac{y_t^2}{4} + \frac{3g^2 + g'^2}{16} + N_s \frac{\lambda_{hs}}{24} \right) T^2, \quad (7)$$

where  $y_t$ ,  $g$ ,  $g'$  are the top Yukawa coupling,  $SU(2)$  gauge coupling and  $U(1)$  gauge coupling, respectively. When  $\lambda_{hs} < 0$  and  $N_s$  is large enough,  $\Pi_h$  may become negative. As a result, the electroweak symmetry can be broken in high temperature.

Another way to realize the electroweak SNR is to add  $N_f$  new singlet fermions  $\chi$ , which interact with the SM Higgs through a five-dimension operator  $\frac{1}{\Lambda} h^2 \bar{\chi} \chi$  as shown in Eq. (1). Thus, the mass of  $\chi$  reads

$$m_\chi(h) = m_\chi^{(0)} - \frac{1}{\Lambda} h^2, \quad (8)$$

and then we have

$$m_\chi^2(h) \supset -\frac{2m_\chi^{(0)}}{\Lambda} h^2 + \frac{1}{\Lambda^2} h^4. \quad (9)$$

This gives the following thermal correction to the SM Higgs potential:

$$\delta V_{\text{SNR}} \simeq N_f \frac{T^2 m_\chi^2(h)}{12} \supset -\frac{N_f m_\chi^{(0)} T^2 h^2}{6\Lambda} + \frac{N_f T^2 h^4}{12\Lambda^2}. \quad (10)$$

Therefore, the Higgs obtains a negative thermal mass  $-N_f m_\chi^{(0)} T^2 / (3\Lambda)$ , which will lead to the high temperature electroweak SNR.

If Higgs thermal mass  $\Pi_h < 0$ ,  $N_f$  must satisfy the condition

$$N_f > \frac{3\Lambda}{m_\chi^{(0)}} \left( \frac{\lambda_h}{2} + \frac{y_t^2}{4} + \frac{3g^2 + g'^2}{16} \right) \sim \frac{1.2\Lambda}{m_\chi^{(0)}}. \quad (11)$$

In order to ensure the rationality of high-temperature expansion in the effective potential, we have [24]

$$T < \frac{\Lambda}{\sqrt{N_f}}. \quad (12)$$

Combining Eqs. (11) and (12), we obtain the maximal temperature of SNR:

$$T_{\text{max}} \sim \sqrt{\frac{\Lambda m_\chi^{(0)}}{1.2}}. \quad (13)$$

In the present work, we adopt the second way to realize the high temperature electroweak SNR. With the leading-order thermal corrections and high temperature approximation, the finite temperature effective potential for our model reads [25,29]

$$V(h_1, h_2, T) \approx -\frac{\mu_{h_1}^2(T)}{2} h_1^2 + \frac{\lambda_{h_1}}{4} h_1^4 + \frac{\mu_{h_2}^2(T)}{2} h_2^2 + \frac{\lambda_{h_2}}{4} h_2^4 + \frac{N_f T^2}{12\Lambda^2} h_2^4 + \frac{\lambda_m}{4} h_1^2 h_2^2, \quad (14)$$

where  $\mu_{h_1}^2(T) = \mu_{h_1}^2 - c_1 T^2$  and  $\mu_{h_2}^2(T) = \mu_{h_2}^2 + c_2 T^2$  with

$$c_1 = \frac{y_t^2}{4} + \frac{\lambda_{h_1}}{2} + \frac{3g^2 + g'^2}{16} + \frac{\lambda_m}{6}, \quad (15)$$

$$c_2 = \frac{\lambda_{h_2}}{2} + \frac{3g^2 + g'^2}{16} + \frac{\lambda_m}{6} - \frac{N_f m_\chi^{(0)}}{3\Lambda}. \quad (16)$$

TABLE I. Parameters for the benchmark point.

$\mu_{h_2}$ (GeV)	$\lambda_{h_2}$	$\lambda_m$	$N_f$	$m_\chi^{(0)}$ (GeV)	$\Lambda$ (GeV)	$T_n$ (GeV)	$\alpha$	$\beta/H_n$
20.71	0.002	0.423	9	187	1361	60	1.33	1177

## IV. PHASE TRANSITION AND GRAVITATIONAL WAVES

### A. First order electroweak phase transition

In this section, we discuss the phase transition from the second Higgs vacuum  $(0, h_2)$  to the SM electroweak vacuum  $(h_1, 0)$  for the benchmark point in Table I. Figure 1 shows the field values as a function of temperature at vacuum  $(h_1, 0)$  (blue line) and  $(0, h_2)$  (orange line). At high temperature, the five-dimension operator  $\frac{1}{\Lambda} |H_2|^2 \bar{\chi} \chi$  can contribute a large negative thermal mass to  $H_2$ . As a result, the electroweak symmetry is broken at high temperature and the Universe is located at vacuum  $(0, h_2)$ . With the decrease of temperature, another local minimum  $(h_1, 0)$  appears at  $T \sim 113$  GeV. When temperature drops to  $T = T_n = 60$  GeV, vacuum  $(0, h_2)$  becomes metastable and it will tunnel to electroweak vacuum  $(h_1, 0)$ , which is the global minimum of scalar potential Eq. (14) as shown in Fig. 2. This process is a first order phase transition which proceeds through the nucleations, collisions and coalescences of the electroweak vacuum bubbles. The bubble nucleation is related to the tunneling from a false vacuum to the true vacuum. The tunneling rate per unit time per unit volume is given by [33]

$$\Gamma(T) \simeq T^4 \left( \frac{S_3}{2\pi T} \right)^{3/2} e^{-S_3/T}, \quad (17)$$

where  $S_3$  is the three-dimensional Euclidean action

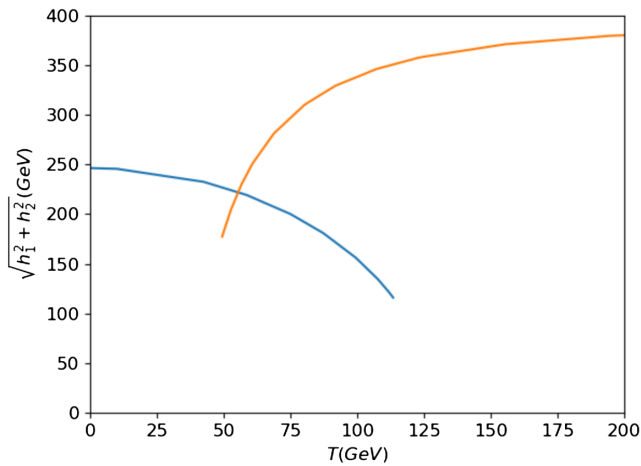


FIG. 1. The field values as a function of temperature at vacuum  $(h_1, 0)$  (blue line) and  $(0, h_2)$  (orange line) for the benchmark point in Table I.

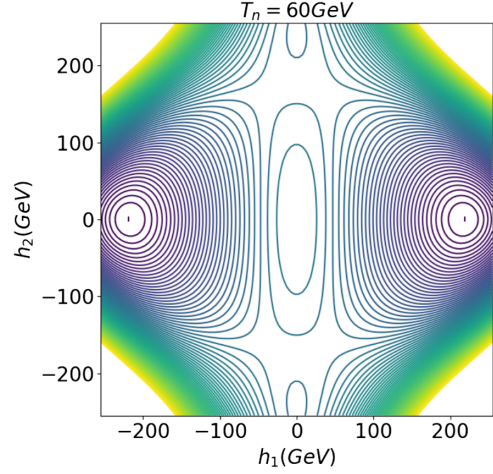


FIG. 2. The potential contours at nucleation temperature  $T_n = 60$  GeV for the benchmark point in Table I.

$$S_3 = \int_0^\infty dr r^2 \left[ \frac{1}{2} \left( \frac{dh(r)}{dr} \right)^2 + V(h, T) \right], \quad (18)$$

which gives the equation of motion

$$\frac{d^2 h}{dr^2} + \frac{2}{r} \frac{dh}{dr} = \frac{dV(h, T)}{dh}. \quad (19)$$

The bounce boundary conditions read

$$\lim_{r \rightarrow \infty} h(r) = 0, \quad \left. \frac{dh}{dr} \right|_{r=0} = 0. \quad (20)$$

At nucleation temperature  $T_n$ , there is at least one bubble within one Hubble volume

$$N(T_n) = \int_{T_n}^{T_c} \frac{dT}{T} \frac{\Gamma(T)}{H(T)^4} = 1. \quad (21)$$

For a fast phase transition, the integral in Eq. (21) is dominated by  $T_n$ , and thus we have

$$\begin{aligned} \frac{\Gamma(T_n)}{H(T_n)^4} &= \frac{T_n^4}{H(T_n)^4} \left( \frac{S_3}{2\pi T_n} \right)^{3/2} e^{-\frac{S_3}{T_n}} \\ &= \left( \frac{90}{\pi^2 g_\star} \right)^2 \frac{M_{\text{pl}}^4}{T_n^4} \left( \frac{S_3}{2\pi T_n} \right)^{3/2} e^{-\frac{S_3}{T_n}} \approx 1, \end{aligned} \quad (22)$$

where  $M_{\text{pl}} = 2.435 \times 10^{18}$  GeV is the reduced Planck mass.  $g_\star = 106.75$  is the relativistic effective degrees of freedom at  $T_n$ .

In present work, we set  $S_3/T_n \sim 140$  and used the public code `CosmoTransitions` [34] to find nucleation temperature  $T_n = 60$  GeV.

## B. Gravitational waves

In this section, we discuss GWs from the first order electroweak phase transition. The GWs mainly come from three aspects: (a) electroweak vacuum bubble collisions [35,36], (b) sound waves in the plasma [37], and (c) magnetohydrodynamic turbulence in the plasma [38,39]. The amplitude of the GWs depends on the energy fraction that released from the phase transition in the total radiation energy density at  $T_n$ , which is given by

$$\alpha = \frac{1}{g_* \pi^2 T_n^4 / 30} \left( \Delta V_T - \frac{T}{4} \frac{\partial \Delta V_T}{\partial T} \right) \Big|_{T_n}. \quad (23)$$

In addition, the duration of the first order electroweak phase transition is also critical to the amplitude of GWs, which is described by  $1/\beta$  with

$$\frac{\beta}{H_n} = T_n \frac{d(S_3/T)}{dT} \Big|_{T_n}. \quad (24)$$

The GWs spectrum today can be expressed as

$$\Omega_{\text{GW}}(f)h^2 \approx \Omega_{\text{col}}(f)h^2 + \Omega_{\text{sw}}(f)h^2 + \Omega_{\text{turb}}(f)h^2, \quad (25)$$

where the contribution from bubble collisions [35]

$$\Omega_{\text{col}}(f)h^2 = 1.67 \times 10^{-5} \left( \frac{H_n}{\beta} \right)^2 \left( \frac{\kappa_{\text{col}} \alpha}{1 + \alpha} \right)^2 \left( \frac{100}{g_*} \right)^{\frac{1}{3}} \times \left( \frac{0.11 v_w^3}{0.42 + v_w^2} \right) \left[ \frac{3.8 (f/f_{\text{col}})^{2.8}}{1 + 2.8 (f/f_{\text{col}})^{3.8}} \right]. \quad (26)$$

Here  $v_w$  stands for the expanding bubble wall velocity, and  $\kappa_{\text{col}}$  is the efficiency factor that describes how much phase transition latent heat is converted into the energy of the wall.  $\kappa_{\text{col}}$  is the functions of  $\alpha$  and it can be written as [40]

$$\kappa_{\text{col}} \simeq \frac{0.7\alpha + 0.2\sqrt{\alpha}}{1 + 0.7\alpha}. \quad (27)$$

$f_{\text{col}}$  is the peak frequency produced by bubble collisions. Taking into account the GW redshift, the peak frequency today is

$$f_{\text{col}} = 16.5 \times 10^{-6} \text{ Hz} \left( \frac{0.62}{1.8 - 0.1 v_w + v_w^2} \right) \quad (28)$$

$$\times \left( \frac{\beta}{H_n} \right) \left( \frac{T_n}{100 \text{ GeV}} \right) \left( \frac{g_*}{100} \right)^{1/6}. \quad (29)$$

The sound waves spectrum has the form [37]

$$\Omega_{\text{sw}}(f)h^2 = 2.65 \times 10^{-6} \frac{1}{\beta/H_n} \left( \frac{\kappa_v \alpha}{1 + \alpha} \right)^2 \left( \frac{g_*}{100} \right)^{-1/3} \times v_w \left( \frac{f}{f_{\text{sw}}} \right)^3 \left( \frac{7}{4 + 3(f/f_{\text{sw}})^2} \right)^{7/2}, \quad (30)$$

where

$$f_{\text{sw}} = 1.9 \times 10^{-5} \text{ Hz} \times \frac{\beta/H_n}{v_w} \left( \frac{T_n}{100 \text{ GeV}} \right) \left( \frac{g_*}{100} \right)^{1/6}, \quad (31)$$

and  $\kappa_v$  is the efficiency factor about the sound waves. In this work, we adopt supersonic deflagrations namely  $c_s < v_w < v_J$ . Here  $c_s$  stands for the sound speed and  $v_J$  corresponds to the Jouguet detonations [41]

$$v_J = \frac{\sqrt{\frac{2}{3}\alpha + \alpha^2} + \sqrt{1/3}}{1 + \alpha}. \quad (32)$$

For  $c_s < v_w < v_J$ , the efficiency factor  $\kappa_v$  can be written as [41]

$$\kappa_v \simeq \kappa_B + (v_w - c_s)\delta\kappa + \frac{(v_w - c_s)^3}{(v_J - c_s)^3} \times [\kappa_C - \kappa_B - (v_J - c_s)\delta\kappa], \quad (33)$$

with

$$\begin{aligned} \kappa_B &\simeq \frac{\alpha^{2/5}}{0.017 + (0.997 + \alpha)^{2/5}}, \\ \kappa_C &\simeq \frac{\sqrt{\alpha}}{0.135 + \sqrt{0.98 + \alpha}}, \\ \delta\kappa &\simeq -0.9 \log \frac{\sqrt{\alpha}}{1 + \sqrt{\alpha}}. \end{aligned} \quad (34)$$

Finally, taking into account the finite duration of the sound wave period, we need to add a factor  $\Upsilon(\tau_{\text{sw}})$  in Eq. (30), where  $\tau_{\text{sw}}$  is given by [42]

$$\tau_{\text{sw}} = \min \left\{ \frac{1}{H_n}, \frac{v_w (8\pi)^{1/3}}{\beta \bar{U}_f} \right\}, \quad \bar{U}_f = \sqrt{\frac{3}{4} \frac{\kappa_v \alpha}{1 + \alpha}}, \quad (35)$$

and factor  $\Upsilon$  reads [43]

$$\Upsilon = 1 - \frac{1}{\sqrt{1 + 2\tau_{\text{sw}} H_n}}. \quad (36)$$

The turbulence spectrum is [38,39]

$$\Omega_{\text{turb}}(f)h^2 = 3.35 \times 10^{-4} \frac{v_w}{\beta/H_n} \left( \frac{\kappa_{\text{turb}} \alpha}{1 + \alpha} \right)^{3/2} \left( \frac{g_*}{100} \right)^{-1/3} \times \frac{(f/f_{\text{turb}})^3}{[1 + (f/f_{\text{turb}})]^{11/3} (1 + 8\pi f/h_*)}, \quad (37)$$

where the efficiency factor  $\kappa_{\text{turb}}$  is unknown and we take  $\kappa_{\text{turb}} \approx (5 \sim 10)\% \kappa_v$  [37]. The peak frequency  $f_{\text{turb}}$  is

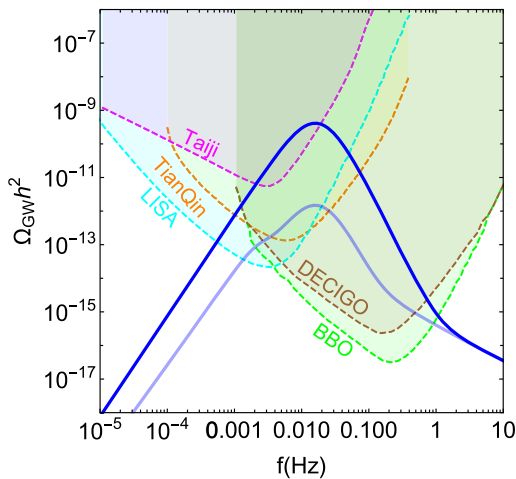


FIG. 3. Sensitivities of GW detectors and GW spectrum for the benchmark point in Table I with  $v_w = 0.85$ . The dark and light blue solid lines represent the total GW energy spectrum without factor  $\Upsilon$  and with factor  $\Upsilon$ , respectively.

$$f_{\text{turb}} = 2.7 \times 10^{-5} \text{ Hz} \times \frac{\beta/H_n}{v_w} \left( \frac{T_n}{100 \text{ GeV}} \right) \left( \frac{g_*}{100} \right)^{1/6}, \quad (38)$$

and

$$h_* = 16.5 \times 10^{-6} \text{ Hz} \left( \frac{T_n}{100 \text{ GeV}} \right) \left( \frac{g_*}{100} \right)^{1/6}. \quad (39)$$

Figure 3 shows the sensitivities of GW detectors and GW spectrum for the benchmark point in Table I. Here we set

the bubble wall velocity  $v_w = 0.85$ . The dark and light blue solid lines represent the GW energy spectrum without factor  $\Upsilon$  and with factor  $\Upsilon$ , respectively. The dashed lines are the power-law integrated sensitivity curves for the Taiji [44], LISA [45,46], TianQin [47], BBO [48], DECIGO [49,50]. It is clear that the GW generated during the first order electroweak phase transition is expected to be observed by LISA, TianQin, Taiji, DECIGO, and BBO.

## V. SUMMARY AND CONCLUSIONS

In this work, we have shown the high temperature electroweak SNR can be realized by introducing  $N_f = 9$  new singlet fermions in 2HDM. These fermions interact with the second Higgs  $H_2$  through a five-dimension operator and they can contribute a negative thermal mass to  $H_2$ , which breaks the electroweak symmetry at high temperature. In this scenario, the Universe is located at vacuum  $(0, h_2)$  above the electroweak scale. With the decrease of temperature, the electroweak vacuum  $(h_1, 0)$  appears and finally becomes the physical vacuum at  $T = T_n = 60 \text{ GeV}$ . We find the SM electroweak phase transition is the first order and the GWs emitted during this process can be detected by future GW experiments such as LISA, TianQin, DECIGO, and BBO, which may provide a smoking gun for the existence of this exotic thermal history of the early Universe.

## ACKNOWLEDGMENTS

This work is supported by Scientific Research Foundation of Inner Mongolia University under Grant No. 10000-22311201/036.

- 
- [1] B. P. Abbott *et al.* (LIGO Scientific and Virgo Collaborations), *Phys. Rev. Lett.* **116**, 061102 (2016).
  - [2] C. Caprini and D. G. Figueroa, *Classical Quantum Gravity* **35**, 163001 (2018).
  - [3] N. Bartolo *et al.*, *J. Cosmol. Astropart. Phys.* **12** (2016) 026.
  - [4] P. Auclair *et al.*, *J. Cosmol. Astropart. Phys.* **04** (2020) 034.
  - [5] C. Caprini *et al.*, *J. Cosmol. Astropart. Phys.* **04** (2016) 001.
  - [6] C. Caprini *et al.*, *J. Cosmol. Astropart. Phys.* **03** (2020) 024.
  - [7] J. R. Espinosa, T. Konstandin, and F. Riva, *Nucl. Phys.* **B854**, 592 (2012).
  - [8] S. Weinberg, *Phys. Rev. D* **9**, 3357 (1974).
  - [9] R. N. Mohapatra and G. Senjanovic, *Phys. Rev. Lett.* **42**, 1651 (1979).
  - [10] Y. Fujimoto and S. Sakakibara, *Phys. Lett.* **151B**, 260 (1985).
  - [11] G. R. Dvali, A. Melfo, and G. Senjanovic, *Phys. Rev. Lett.* **75**, 4559 (1995).
  - [12] P. Salomonson, B. S. Skagerstam, and A. Stern, *Phys. Lett.* **151B**, 243 (1985).
  - [13] G. Bimonte and G. Lozano, *Phys. Lett. B* **366**, 248 (1996).
  - [14] G. R. Dvali, A. Melfo, and G. Senjanovic, *Phys. Rev. D* **54**, 7857 (1996).
  - [15] J. Orloff, *Phys. Lett. B* **403**, 309 (1997).
  - [16] M. B. Gavela, O. Pene, N. Rius, and S. Vargas-Castrillon, *Phys. Rev. D* **59**, 025008 (1999).
  - [17] A. Ahriche, arXiv:1003.5045.
  - [18] J. R. Espinosa, M. Losada, and A. Riotto, *Phys. Rev. D* **72**, 043520 (2005).
  - [19] B. Bajc and G. Senjanovic, *Phys. Rev. D* **61**, 103506 (2000).
  - [20] P. Agrawal and M. Nee, *J. High Energy Phys.* **10** (2021) 105.
  - [21] P. Meade and H. Ramani, *Phys. Rev. Lett.* **122**, 041802 (2019).
  - [22] I. Baldes and G. Servant, *J. High Energy Phys.* **10** (2018) 053.

- [23] A. Glioti, R. Rattazzi, and L. Vecchi, *J. High Energy Phys.* **04** (2019) 027.
- [24] O. Matsedonskyi and G. Servant, *J. High Energy Phys.* **09** (2020) 012.
- [25] O. Matsedonskyi, *J. High Energy Phys.* **04** (2021) 036.
- [26] M. Carena, C. Krause, Z. Liu, and Y. Wang, *Phys. Rev. D* **104**, 055016 (2021).
- [27] T. Biekötter, S. Heinemeyer, J. M. No, M. O. Olea, and G. Weiglein, *J. Cosmol. Astropart. Phys.* **06** (2021) 018.
- [28] Y. Bai, S. J. Lee, M. Son, and F. Ye, *J. High Energy Phys.* **07** (2021) 225.
- [29] O. Matsedonskyi, J. Unwin, and Q. Wang, *J. High Energy Phys.* **12** (2021) 167.
- [30] W. Chao, H.-K. Guo, and X.-F. Li, [arXiv:2112.13580](https://arxiv.org/abs/2112.13580).
- [31] J. H. Chang, M. O. Olea-Romacho, and E. H. Tanin, *Phys. Rev. D* **106**, 113003 (2022).
- [32] O. Matsedonskyi, J. Unwin, and Q. Wang, *J. High Energy Phys.* **02** (2023) 198.
- [33] M. S. Turner, E. J. Weinberg, and L. M. Widrow, *Phys. Rev. D* **46**, 2384 (1992).
- [34] C. L. Wainwright, *Comput. Phys. Commun.* **183**, 2006 (2012).
- [35] S. J. Huber and T. Konstandin, *J. Cosmol. Astropart. Phys.* **09** (2008) 022.
- [36] Y. Di, J. Wang, R. Zhou, L. Bian, R.-G. Cai, and J. Liu, *Phys. Rev. Lett.* **126**, 251102 (2021).
- [37] M. Hindmarsh, S. J. Huber, K. Rummukainen, and D. J. Weir, *Phys. Rev. D* **92**, 123009 (2015).
- [38] P. Binetruy, A. Bohe, C. Caprini, and J.-F. Dufaux, *J. Cosmol. Astropart. Phys.* **06** (2012) 027.
- [39] C. Caprini, R. Durrer, and G. Servant, *J. Cosmol. Astropart. Phys.* **12** (2009) 024.
- [40] M. Kamionkowski, A. Kosowsky, and M. S. Turner, *Phys. Rev. D* **49**, 2837 (1994).
- [41] J. R. Espinosa, T. Konstandin, J. M. No, and G. Servant, *J. Cosmol. Astropart. Phys.* **06** (2010) 028.
- [42] J. Ellis, M. Lewicki, and J. M. No, *J. Cosmol. Astropart. Phys.* **07** (2020) 050.
- [43] H.-K. Guo, K. Sinha, D. Vagie, and G. White, *J. Cosmol. Astropart. Phys.* **01** (2021) 001.
- [44] W.-H. Ruan, Z.-K. Guo, R.-G. Cai, and Y.-Z. Zhang, *Int. J. Mod. Phys. A* **35**, 2050075 (2020).
- [45] P. Amaro-Seoane *et al.* (LISA Collaboration), [arXiv:1702.00786](https://arxiv.org/abs/1702.00786).
- [46] M. Breitbach, J. Kopp, E. Madge, T. Opferkuch, and P. Schwaller, *J. Cosmol. Astropart. Phys.* **07** (2019) 007.
- [47] J. Mei *et al.* (TianQin Collaboration), *Prog. Theor. Exp. Phys.* **2021**, 05A107 (2021).
- [48] C. Cutler and J. Harms, *Phys. Rev. D* **73**, 042001 (2006).
- [49] H. Kudoh, A. Taruya, T. Hiramatsu, and Y. Himemoto, *Phys. Rev. D* **73**, 064006 (2006).
- [50] M. Musha (DECIGO Working group), *Proc. SPIE Int. Soc. Opt. Eng.* **10562**, 105623T (2017).